Relative importance of methylotrophic methanogenesis in sediments of the Western Mediterranean Sea

Guang-Chao Zhuang [a,b,*], Verena B. Heuer [a], Cassandre S. Lazar [a,c], Tobias Goldhammer [a,1], Jenny Wendt [a], Vladimir A. Samarkin [b,2], Marcus Elvert [a], Andreas P. Teske [c], Samantha B. Joye [b], Kai-Uwe Hinrichs [a]

[a] *MARUM Center for Marine Environmental Sciences, University of Bremen, 28359 Bremen, Germany*
[b] *Department of Marine Sciences, University of Georgia, 30602 Athens, GA, USA*
[c] *Department of Marine Sciences, University of North Carolina at Chapel Hill, Chapel Hill, 27599 NC, USA*

Received 15 June 2017; accepted in revised form 25 December 2017; available online 3 January 2018

Abstract

Microbial production of methane is an important terminal metabolic process during organic matter degradation in marine sediments. It is generally acknowledged that hydrogenotrophic and acetoclastic methanogenesis constitute the dominant pathways of methane production; the importance of methanogenesis from methylated compounds remains poorly understood. We conducted various biogeochemical and molecular genetic analyses to characterize substrate availability, rates of methanogenesis, and methanogen community composition, and further evaluated the contribution of different substrates and pathways for methane production in deltaic surface and subsurface sediments of the Western Mediterranean Sea. Major substrates representing three methanogenic pathways, including H_2, acetate, and methanol, trimethylamine (TMA), and dimethylsulfide (DMS), were detected in the pore waters and sediments, and exhibited variability over depth and between sites. In accompanying incubation experiments, methanogenesis rates from various ^{14}C labeled substrates varied as well, suggesting that environmental factors, such as sulfate concentration and organic matter quality, could significantly influence the relative importance of individual pathway. In particular, methylotrophic and hydrogenotrophic methanogenesis contributed to the presence of micromolar methane concentrations in the sulfate reduction zone, with methanogenesis from methanol accounting for up to 98% of the total methane production in the topmost surface sediment. In the sulfate-depleted zone, hydrogenotrophic methanogenesis was the dominant methanogenic pathway (67–98%), and enhanced methane production from acetate was observed in organic-rich sediment (up to 31%). Methyl coenzyme M reductase gene (*mcrA*) analysis revealed that the composition of methanogenic communities was generally consistent with the distribution of methanogenic activity from different substrates. This study provides the first quantitative assessment of methylotrophic methanogenesis in marine sediments and has important implications for marine methane cycling. The occurrence of methylotrophic methanogenesis in surface sediments could fuel the anaerobic oxidation of methane (AOM) in the shallow sulfate reduction zone. Release of methane

* Corresponding author at: Department of Marine Sciences, University of Georgia, 325 Sanford Dr., Athens, GA, USA.
E-mail address: gzhuang@uga.edu (G.-C. Zhuang).
[1] Current address: Leibniz Institute for Freshwater Ecology and Inland Fisheries, Department of Chemical Analytics and Biogeochemistry, Berlin, Germany.
[2] Deceased.

https://doi.org/10.1016/j.gca.2017.12.024

produced from methylotrophic methanogenesis could be a source of methane efflux to the water column, thus influencing the benthic methane budgets.

Keywords: Methylotrophic methanogenesis; Methanogenesis rate; Methylated substrates; *mcrA*; Sulfate-reducing sediment; Rhône Delta; Molouya Delta; Gulf of Lions; Western Mediterranean Sea; Deep biosphere; Early diagenesis

1. INTRODUCTION

Methane is a potent greenhouse gas, and marine sediments are the largest global reservoir of methane (Milkov, 2004). Much of the methane present in marine sediments is generated from microbial methanogenesis during organic matter degradation. Methanogenic archaea produce methane from a limited number of substrates (e.g., bicarbonate, acetate, methylated compounds) that are generated during the hydrolysis, depolymerization, and fermentation of large organic macromolecules. Despite their limited substrate range, methanogens are phylogenetically diverse and span different orders within the Euryarchaeota phylum of the Archaea (Liu and Whitman, 2008; Iino et al., 2013), yet uncultured methanogens also putatively exist in the phyla Bathyarchaeota (Evans et al., 2015) and Verstraetearchaeota (Vanwonterghem et al., 2016).

Despite of the large quantities of methane observed in marine sediments and the fairly extensive knowledge of the specific processes and microorganisms dominating methane production, surprisingly little is known about alternative methanogenic pathways. Acetoclastic and hydrogenotrophic methanogenesis are often considered the principal pathways of methanogenesis, but both of these pathways can be inhibited thermodynamically by sulfate reduction. As a result, these processes occur mainly in deeper sediments, below the sulfate reduction zone (Valentine, 2011), where methanogens no longer need to compete for H_2 and acetate with sulfate-reducing bacteria (Oremland et al., 1982; King et al., 1983). In contrast, methylotrophic methanogens can be competitive when they compete with sulfate reducers for methylated substrates (e.g., methanol, methylamines, or other C1-compounds). Facilitated by utilization of those methylated substrates, sulfate reduction and methanogenesis were observed to co-occur in salt marsh sediment (Oremland et al., 1982). The concurrence of sulfate reduction and methanogenesis due to methylotrophic methanogenesis was also postulated in deep marine subseafloor sediments (Mitterer et al., 2001). Recently, methylotrophic methanogenesis was identified as the dominant methanogenic pathway in hypersaline sediment of Orca Basin, Gulf of Mexico (Zhuang et al., 2016). Only a few studies on methylotrophic methanogenesis have been conducted *in vitro* in salt marsh or intertidal sediments (King et al., 1983; Parkes et al., 2012; Chuang et al., 2016), where sulfate concentrations are high and methylated substrates such as methylamines are abundant (King, 1988; Wang and Lee, 1994). The contribution of methylated compounds to methane production in marine surface and subsurface sediment remains elusive.

Typical organic-rich marine sediments are geochemically stratified with a clear transition from sulfate- to methane-bearing sediments, termed the sulfate methane transition zone, hereafter SMTZ. However, methane is virtually ubiquitous at ~micromolar concentrations within the sulfate reduction zone (e.g., D'Hondt et al., 2004; Valentine, 2011). The occurrence of *in situ* methane production in the sulfate-reducing zone rather than diffusive flux from underlying horizons in sediments from Santa Barbara Basin, Cariaco Basin and Skan Bay is supported by the methane's higher radiocarbon content relative to more deeply buried sediments from the methanogenic zone (Kessler et al., 2008). Considerable methanogenic activity has been observed in *in vitro* incubations of sediments from the sulfate reduction zone (e.g., Xie et al., 2013), which also indicates the presence of active methanogens and suggests a potential for methane production in sulfate-reducing environments. Increasing evidence further suggests microbial methanogenesis in the surface sediment could be a source of methane to the water column (Maltby et al., 2016; Chronopoulou et al., 2017). Nevertheless, the mechanisms and magnitude of methane production in these surface or sulfate-reducing sediments remain poorly understood.

To decipher the role of methylotrophic methanogenesis, and examine the relative importance of methanogenic pathways and controlling factors, we present here the first comprehensive evaluation of methane production from different substrates in marine sediments. A suite of biogeochemical and molecular genetic analyses was conducted in surface and subsurface sediment from the Western Mediterranean Sea. Potential methanogenic substrates such as H_2, acetate, methanol, trimethylamine (TMA), dimethylsulfide (DMS) or dimethylsulfoniopropionate (DMSP) were collectively characterized in the pore water and solid phase of the sediments, and the resultant methanogenic activities and communities were combined to estimate the magnitude of methanogenesis and delineate the importance of different substrates fueling the process. Previous studies have proposed the significant impact of organic carbon transport and deposition on the benthic microbial communities and biogeochemical processes in the sediments of this area (e.g., Canals et al., 2006; Fagervold et al., 2014). Therefore, we selected our study sites representing different depositional and geochemical settings (e.g., in the delta and on the shelf or along the gradient of terrestrial organic matter) (Heuer et al., 2014), to elucidate the influence of environmental factors on the relative importance of individual methanogenic pathways.

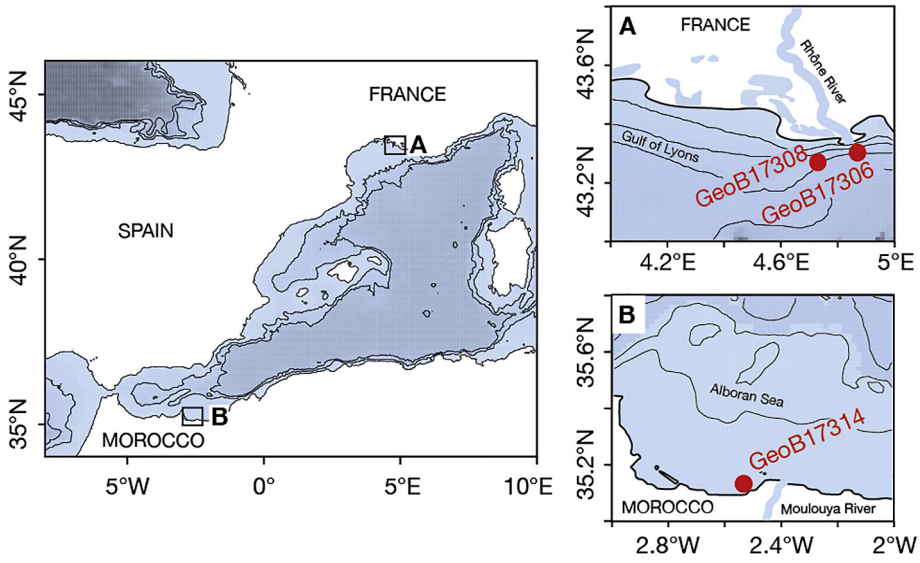

Fig. 1. Sampling sites in the Western Mediterranean Sea. Panel A: Rhône Delta sites GeoB17306 and GeoB17308, Panel B: Moulouya Delta Site GeoB17314. Isobath distances are 1000 m on the large overview map, 10 m on Panel A, and 250 m on Panel B. The maps were created using the R package marmap (Pante and Simon-Bouhet, 2013).

2. MATERIALS AND METHODS

2.1. Site description and sampling protocol

Sediment cores were retrieved during expedition POS450 of the research vessel *Poseidon* offshore the Rhône River (France) and Moulouya River (Morocco) in the Western Mediterranean Sea in April 2013 (Fig. 1). Site GeoB17306 was located in the prodelta of the Rhône River while GeoB17308 was established 12 km off the river mouth. Site GeoB17314 was located on the shelf off the Moulouya River. Surface sediments were recovered by multi-corer (MUC), and deeper sediments were retrieved by gravity corer (see Table 1 for details). More details on sites and sampling procedures are given in Heuer et al. (2014). The geochemical data of this study are archived in PANGAEA–Data Publisher for Earth & Environmental Science (https://doi.pangaea.de/10.1594/PANGAEA.883599).

After retrieval, the MUC sediment core was sectioned immediately on board at ambient temperatures around 13 °C using a core extruder. For methane analysis, 2–3 mL sediment were taken from the freshly cut sediment surface and transferred with a 5 mL cut-off syringe into a helium-purged 22 mL serum vial, which was closed with a Teflon septum and crimp-capped. Methane concentrations were determined on-board the ship within two days after collection (see next section). Another set of samples was collected similarly, fixed by addition of 5 mL 1 M NaOH, and stored at 4 °C for shore-based isotopic analysis of methane. For hydrogen analysis, a sediment sample of 2–3 mL was extruded into a 12-mL headspace vial, immediately sealed with a thick black butyl stopper, crimp capped, and flushed with N_2 (purity = 99.999%) for at least 1 min (Lin et al., 2012). Samples were stored at 4 °C for shore-based incubation and analysis. Subsamples of sediments for analysis of total organic carbon (TOC), TMA, DMS or DMSP in the solid phase were collected using cut-off plastic syringes, transferred to headspace vials, and stored at −20 °C. Pore water samples were extracted from sediment via Rhizon soil moisture samplers (0.1 μm porous polymer, Rhizosphere Research, Wageningen, the Netherlands) (Seeberg-Elverfeldt et al., 2005). Rhizons were rinsed with at least 30 mL of dilute hydrochloric acid (pH 1–2) followed by 30 mL of Milli-Q water before use. The collected pore waters were split into aliquots for analyses of sulfate,

Table 1
Overview of sampling sites in the Western Mediterranean Sea.

Site	Location	Latitude	Longitude	Core type	Core length (cm)	Water depth (m)	Sedimentation rate (cm/a)
GeoB17306	Rhône River pro-delta	43°18.95′ N	4°52.18′ E	Gravity Core	516	30	35[a]
GeoB17308	Gulf of Lions shelf	43°16.20′ N	4°43.79′ E	Gravity Core	405	62	0.65[a]
GeoB17314	Shelf offshore the Moulouya River	35°7.99′ N	2°31.98′ W	Multicore	35	66	n.d.[b]

[a] Miralles et al. (2005).
[b] Sedimentation rates were not available at Site GeoB17314.

acetate, dissolved inorganic carbon (DIC), volatile alcohols, TMA, DMS and stored at −20 °C.

Gravity cores were cut into 1 m segments on deck, processed immediately in the shipboard laboratory at an ambient temperature of 18 °C, i.e. 5 °C above *in situ* temperature, or stored temporally at 7 °C. In order to minimize degassing and oxygenation of the sediment, core liners were left intact during pore water and gas sampling, which were conducted first. Syringe samples for solid phase analysis (e.g., methane, hydrogen, TMA, DMSP) were taken from freshly exposed sediments through small sampling ports (ca. 2 cm × 3 cm), which were cut into the sealed core liners. Pore water samples were extracted with Rhizons from holes drilled into the core liner, and stored in the same manner as those collected from the MUC core.

For methanogenesis rate measurements, ~3 mL sediments were introduced into the cut-end Hungate tubes, and a plunger modified from the butyl rubber stopper was added from the cut end to move the sediment to the threaded end of the tube (Bowles et al., 2011). Then the septum was placed onto the sediment without headspace, and the screw cap was tightened. The gas-tight sample tubes filled with sediments were stored at 4 °C before incubation with radiotracers. Quadruplicate samples (triplicate samples plus a killed control) for each substrate (HCO_3^-, acetate, methanol, methylamine) were collected at various depths from Sites GeoB17306, GeoB17308, and GeoB17314. Activity in killed control samples was terminated by injecting 2.5 mL of 2 M NaOH into the sediment before commencing the incubation.

Sediments for DNA analysis were sampled with cut-off syringes, stored in sterile Falcon tubes, immediately frozen at −32 °C (this was the coldest temperature available), shipped on dry ice, and then stored at −80 °C in the laboratory at UNC in Chapel Hill, NC, U.S.A., before analysis.

2.2. Biogeochemical analyses

Concentrations of dissolved methane were measured on board on a gas chromatograph (Trace GC Ultra, ThermoFinnigan) equipped with a CP-PoraBOND Q (Varian Inc.) column and a flame ionization detector (FID) as described previously (Ertefai et al., 2010); using manual injection of 100–500 µL headspace gas. Analysis of $\delta^{13}C$ values of methane was performed on a gas chromatography combustion isotope ratio mass spectrometry (GC-C-IRMS) system combining a ThermoFinnigan Trace GC Ultra with a DELTA Plus XP mass spectrometer via a ThermoFinnigan GC Combustion III interface as described previously (Ertefai et al., 2010). Sulfate concentrations were determined by ion chromatography (Metrohm 861 Advanced Compact IC, column A Supp 5, conductivity detection after chemical suppression) as described previously (Goldhammer et al., 2011). Quantitative and isotopic analyses of volatile fatty acids (VFAs) in the pore water were performed with a liquid chromatography-isotope ratio mass spectrometry system, which consisted of a ThermoFinnigan Surveryor high performance liquid chromatography (HPLC) equipped with a VA Nucleogel Sugar 810-H column (300 × 7.8 mm; Macherey-Nagel, Germany) and a guard column of the same material coupled in line with a DELTA Plus XP IRMS via a ThermoFinnigan LC Isolink interface (Heuer et al., 2006, 2009).

Methanol and ethanol in pore water was determined by a custom-built purge and trap pre-treatment system connected to a Hewlett-Packard GC 5890 series II equipped with a FID and Alltech Heliflex® AT-Q capillary column (30 m × 0.32 mm I.D.; Alltech Associates, Inc., Deerfield, US) (Zhuang et al., 2014). The dissolved pool of DMS and DMSP (hereafter, $DMS(P)_d$), and dissolved TMA in the pore water were measured in one analytical step, and total base-hydrolysable DMS and DMSP (hereafter $DMS(P)_T$) as well as base-extractable TMA in the sediment were quantified simultaneously (Zhuang et al., 2017). Briefly, $DMS(P)_d$ and TMA in the pore water, or base-hydrolysable $DMS(P)_T$ and TMA in the sediment, were released by the addition of NaOH, pre-concentrated with a purge and trap procedure, and analyzed on a Trace GC 2000 (Thermo Finnigan, Milan, Italy) coupled to a DSQ II MS (Thermo Finnigan, Texas, USA) with a Rtx®-Volatile Amine Column (30 m × 0.32 mm I.D., Restek GmbH, Homburg, Germany). The detection limits for DMS and TMA were 0.1 and 20 nM, respectively. To quantify exchangeable TMA that reversibly adsorbs to exchange sites on sediment particles (Lee and Olson, 1984; Wang and Lee, 1990), ~4 g wet sediment was extracted with 20 mL 1 M LiCl for 2 h with continuous agitation. After centrifugation, the supernatant was treated with the same procedure for TMA analysis in the pore water.

Determinations of TOC and $\delta^{13}C_{TOC}$ were conducted on pre-weighed, freeze-dried, decarbonatized sediment using a ThermoScientific Flash 2000 elemental analyzer coupled to a ThermoScientific DELTA V Plus IRMS via a ThermoScientific ConFlo IV interface (Schmidt et al., 2017). DIC in pore water samples fixed with zinc chloride was measured by carbon dioxide infrared spectroscopy on a carbon analyzer (multi N/C® 2100s, Analytik Jena, Germany). Carbon dioxide was stripped from the sample in a 10% phosphoric acid trap. The carbon isotopic composition of DIC was analyzed using a gasbench coupled to a Finnigan MAT 252 mass spectrometer (Heuer et al., 2010). Headspace hydrogen concentrations were measured after 45 days of incubation with a Peak Performer 1 Reduced Gas Analyzer equipped with a mercury oxide detector (Peak Laboratories, USA) following the protocol of Lin et al. (2012).

2.3. Methanogenic activity

Methanogenesis rate measurements were conducted using ^{14}C-labeled substrates according to previously described methods (Bowles et al., 2011). Sediment samples in the cut-end Hungate tubes were injected with 100 µL of ^{14}C-bicarbonate (600 kBq), 1, 2-^{14}C-acetate (210 kBq), ^{14}C-methanol (298 kBq) or ^{14}C-methylamine (143 kBq) in sets of four, with one killed control and three live samples; all samples were incubated at *in situ* temperature (i.e., 13 °C) for 7 days. The injection of the ^{14}C-labeled substrates would result in an addition of 91 µM bicarbonate,

32 μM acetate, 45 μM methanol and 22 μM methylamine to the initial samples. We minimized the amount of tracer added so as to minimally alter *in situ* concentrations, but we had to ensure detection of potential activity at the level of label addition. These additions achieved both but in light of this, the measured rates represented the methanogenic potential and might not be identical to the *in situ* rates in the original sediment. However, relative comparisons between sites and depths are valid and environmentally relevant as the added tracers or *in situ* substrate concentrations were of similar magnitude (e.g., acetate, methanol, methylamine). For killed controls, 2.5 mL of 2 M NaOH were injected into the samples and they were homogenized before tracer addition. Incubations were terminated by injecting 2.5 mL 2 M NaOH into the samples using a syringe and needle, and a headspace was created by gently pulling the plunger to the base of the Hungate tube. The methane production rate was determined by quantitatively converting $^{14}CH_4$ in the headspace to $^{14}CO_2$ and trapping the evolved $^{14}CO_2$.

Vessels were shaken vigorously and purged with a gentle flow of CO_2 free compressed air. Volatile ^{14}C-labeled non-methane components such as $^{14}CO_2$, ^{14}C-acetate, ^{14}C-methanol and ^{14}C-methylamine were removed from the gas stream via a series of traps. The gas stream then passed through an 800 °C titanium-nickel alloy column packed with copper oxide to catalyze the conversion of $^{14}CH_4$ to $^{14}CO_2$. The resulting $^{14}CO_2$ was trapped in 4.5 mL ScintiSafe Gel cocktail mixed with 1.5 mL Carbosorb E and quantified on a LS Beckman 6500 liquid scintillation counter. The recovery of the combustion system was >90%, as determined by adding a known activity of $^{14}CH_4$. Methanogenesis rates were calculated using substrate concentrations measured in separate samples, and activities recovered from the $^{14}CH_4$ pool (Eq. (1)):

$$\text{MOG rate} = C_{substrate} \times \alpha/t(\text{DPM-}^{14}CH_4/\text{DPM-}^{14}C_{substrate}) \quad (1)$$

where MOG is the rate of methanogenesis from bicarbonate, acetate, and methanol (nmol substrate reduced cm^{-3} d^{-1}), $C_{substrate}$ is the concentration of different substrates (nmol cm^{-3}), α is the isotopic fractionation factor (assumed to be 1.04 for bicarbonate, 1.02 for acetate and 1.07 for methanol; Krzycki et al., 1987; Summons et al., 1998; Whiticar, 1999), t is the period of incubation (days), DPM-$^{14}CH_4$ is the activity recovered in the products pool, DPM-$^{14}C_{substrate}$ is the activity of the substrate injected into sample (DPM: disintegrations per minute). Relative turnover times for ^{14}C-labeled substrates were compared and calculated (as *in situ* concentrations were unknown for methylamine) based on the time (in days) required to fully metabolize the total amount of added ^{14}C-substrate to methane (Eq. (2)):

$$\text{Turnover time} = \text{DPM-}^{14}C_{substrate}/(\text{DPM-}^{14}CH_4/t) \quad (2)$$

All the rates and turnover time calculations were corrected by subtracting killed sample counts, which were typically close to the instrument blanks.

2.4. Molecular analysis

DNA was extracted from 10 g of sediment using the UltraClean® Mega Soil DNA Isolation Kit (MO BIO, CA). The *mcrA* genes were amplified by PCR using the ME1 (GCMATGCARATHGGWATGTC) and ME2 (TCATKGCRTAGTTDGGRTAGT) primers for methanogens (Hales et al., 1996). The PCR conditions were as follows: denaturation at 94 °C for 40 s, annealing at 50 °C for 1 min 30 s, and extension at 72 °C for 3 min for 30 cycles.

PCR products were cloned using the TOPO XL cloning kit (Invitrogen, CA), and chemically transformed into Escherichia coli TOPO10 One Shot cells according to the manufacturer's instructions. The cloned PCR products were sequenced by Genewiz (South Plainfield, NJ) on an ABI Prism 3730xl sequencer using the M13R primer.

Sequences were analyzed using the NCBI BLASTN search program within GeneBank (http://blast.ncbi.nlm.nih.gov/Blast) (Altschul et al., 1990). The *mcrA* sequences were translated into amino acid sequences using BioEdit and amino acid sequences were aligned using ClustalX (Larkin et al., 2007). Sequence data were analyzed with the MEGA4.0.2 program (Tamura et al., 2007). The phylogenetic trees were calculated by the neighbor-joining analysis. The robustness of inferred topology was tested by 1000 reiterations of bootstrap resampling. The sequence data reported here can be found in the GenBank nucleotide sequence database under the accession numbers: MG777641-MG777944.

3. RESULTS

3.1. Geochemistry at study sites

Generally, the three selected sites displayed different geochemical characteristics (Table 2). At Site GeoB17306 in the prodelta of the Rhône River, the concentrations of sulfate decreased from roughly 30 mM at the surface to 1 mM at 100 cm (Fig. 2A). Methane concentrations were generally low (<0.1 mM) in the sulfate-rich sediment, but increased rapidly to ~5.3 mM at 105 cm and remained high in the deeper sections of the 500 cm long core (Fig. 2A). A clear sulfate-methane transition zone was observed at ~100 cm. The δ^{13}C values of methane increased from −67.2‰ at 14 cm to −55.1‰ at 57 cm, shifted to −62.3‰ at 82 cm, and varied between −73.1‰ and −80.8‰ below 100 cm (Fig. 2B). TOC was relatively abundant (~1.1%) (Fig. 2C) and the stable carbon isotopic composition of TOC (−27.2‰ to −25.8‰) (Fig. 2C) and the C/N ratio (11–19) (Fig. 2D) suggested that organic matter was primarily derived from terrestrial sources (e.g., soil, C3 land plant). A high terrestrial input of organic matter at this site had been previously reported (Tesi et al., 2007).

Sulfate decreased from 31 mM at the surface to 1.4 mM at 270 cm at Site GeoB17308 on the shelf of Gulf of Lions (Fig. 3A). With the depletion of sulfate, methane accumulated progressively and the concentration increased to 3 mM at 403 cm (Fig. 3A). Methane was strongly depleted in ^{13}C below 290 cm, with δ^{13}C values between −89‰ and −97‰ (Fig. 3B). Compared to Site GeoB17306, the TOC

content was much lower (average: 0.5%, Fig. 3C). The $\delta^{13}C$ value of TOC was more positive (~−25.1‰) and its C/N ratio (~9.5) was lower, which was indicative of less terrestrial input and a higher proportion of marine organic matter at Site GeoB17308. This result agreed well with previous findings (Tesi et al., 2007).

In the surface sediment of GeoB17314 on the shelf off the Moulouya River, pore water sulfate varied little with depth, and the concentrations of methane were ~1 μM (Fig. 4A). TOC content generally decreased with depth and the average value of TOC was only 0.2% (Fig. 4B). Ranging from −22.6‰ to −24.0‰ (average: −23.3‰, Fig. 4B), $\delta^{13}C$ values of TOC were indicative for organic matter derived from C4 plants or marine sources. Compared to Sites GeoB17306 and GeoB17308, the C/N ratio was three to four times lower at GeoB17314 (average: 3.1), and slightly deceased from 3.9 at 1.5 cm to 1.4 at 32.5 cm (Fig. 4C).

3.2. Distribution of potential methanogenic substrates

At Site GeoB17306, the concentration of DIC increased from 4.2 mM at 25 cm to a maximum of 42.1 mM at 125 cm, then decreased to 20.1 mM at 175 cm and varied between 22.6 mM and 32.3 mM below 200 cm (Fig. 2E). The $\delta^{13}C$ values of DIC increased from −23.7‰ at 50 cm to 3.8‰ at 500 cm (Fig. 2E). Hydrogen concentrations were generally low and varied between 0.18 and 0.57 nM (Fig. 2F). Acetate concentrations ranged from 1.2 to 5.7 μM, and the $\delta^{13}C$ values of acetate were between −29.8‰ and −32.4‰ in samples, in which concentrations exceeded 5 μM (the lower threshold required for isotopic analysis) (Fig. 2G). The concentrations of methanol and ethanol were generally below 2 μM and 0.5 μM, respectively (Fig. 2H). Dissolved TMA was not detectable in the pore water (detection limit: 20 nM), while exchangeable and base-extractable TMA were relatively abundant though concentrations decreased with depth (exchangeable TMA: 0.3–1.5 μmol kg^{-1}; base-extractable TMA: 0.7–3.2 μmol kg^{-1}, Fig. 2I). Likewise, the pore water concentrations of the dissolved pool of DMS and DMSP ($DMS(P)_d$) were in the low nanomolar range (0.2–2.1 nM; Fig. 2J). Base-hydrolysable $DMS(P)_T$ was three orders of magnitude higher than $DMS(P)_d$, and ranged from 0.2 to 1.8 μmol kg^{-1} (Fig. 2J).

In contrast to GeoB17306, DIC concentrations were much lower at GeoB17308, which increased from 2.8 mM at 20 cm to 6.7 mM at 270 cm, and declined to 1 mM at 345 cm (Fig. 3E). The $\delta^{13}C$ of DIC varied slightly with depth, reached a minimum value of −20.5‰ at 270 cm and became progressively positive until −8.6‰ at 395 cm (Fig. 3E). Hydrogen concentrations were higher at GeoB17308 (0.2–4.9 nM) (Fig. 3F), with a peak observed between 240 cm and 290 cm. The concentration of acetate increased from 2.7 μM at 20 cm to 5.2 μM at 345 cm, and the isotopic values were −25.8‰ at 295 cm and −27.2‰ at 345 cm (Fig. 3G). The average concentration of methanol was 0.2 μM at GeoB17308, much lower than that of GeoB17306 (Fig. 3H). Similarly, TMA was below detection limit in the pore water. The average concentrations of exchangeable and base-extractable TMA were 0.3 μmol kg^{-1} and 0.5 μmol kg^{-1}, respectively (Fig. 3I). Despite the low concentration of $DMS(P)_d$ in the pore water (0.3–1.3 nM; Fig. 3J), base-hydrolysable $DMS(P)_T$ was much more abundant, with an average of 1.2 μmol kg^{-1} in the sediment (Fig. 3J).

In the surface sediment of GeoB17314, DIC concentrations varied between 1.4 mM and 3.0 mM (Fig. 4D). The carbon isotopic values of DIC became increasingly negative with depth below 10 cm, reaching −7.5‰ at 36 cm (Fig. 4D). Hydrogen concentrations generally increased with depth and reached a maximum of 1.6 nM at 32.5 cm (Fig. 4E). The concentrations of acetate ranged from 0.7 to 4.1 μM (Fig. 4F). Methanol was more abundant in the upper 7 cm (maximum: 2.4 μM) and then the concentration decreased with increasing depth (Fig. 4G). $DMS(P)_d$ exhibited a maximum of 3.1 nM at 4 cm and showed a similar trend with concentrations decreasing with depth (Fig. 4I). Exchangeable and base-extractable TMA, and base-hydrolysable $DMS(P)_T$ in the surface sediment of GeoB17314 were much higher than those at GeoB17306 and GeoB17308. The maxima of those pools were found in the uppermost sediment and then the concentrations deceased with depth (exchangeable TMA: 5.9 μmol kg^{-1}; base-extractable TMA: 9.9 μmol kg^{-1}; $DMS(P)_T$: 13.1 μmol kg^{-1}) (Fig. 4H and J).

3.3. Methanogenic activities

To assess the methanogenic activities, methane production rates were measured from key substrates representing different pathways. At the prodelta site GeoB17306, the methanogenic activities from bicarbonate and acetate were low in the upper 70 cm, and the corresponding turnover times (Eq. (2); time required to fully metabolize the injected ^{14}C substrates to methane) of these two substrates were $\sim 1.2 \times 10^6$ days and $\sim 3.1 \times 10^4$ days, respectively (Fig. S1, A and B). In contrast, the turnover of methanol and methylamine was 3–5 orders of magnitude faster, with an average turnover time of 44 and 25 days, respectively (Fig. S1, C and D). Methane production rates from methanol and bicarbonate were relatively high (~0.02 nmol cm^{-3} d^{-1}) in the top 70 cm, both of which were about hundred times the rate of acetoclastic methanogenesis (Fig. 5). Below 90 cm, methanol and methylamine turnover times were similar to those in the surface sediment. The turnover of bicarbonate and acetate increased, with acetate increasing more than bicarbonate and exhibiting a turnover time of only 43 days (Fig. S1, A and B). Methanogenesis from H_2/CO_2 increased to a maximum of 1.83 nmol cm^{-3} d^{-1} at 120 cm and rates remained elevated down to the bottom of the core (Fig. 5A). The average rate of acetoclastic methanogenesis was 0.14 nmol cm^{-3} d^{-1} in the deeper sulfate-depleted sediment (Fig. 5B), about thousand times higher than in overlying sulfate-bearing sediment.

At the shelf site GeoB17308, the turnover times of bicarbonate were lower in the upper 75 cm (3.1×10^5 days) than in the deeper sulfate-bearing zone at 200 cm (1.4×10^7 days), and then decreased progressively to 8.6×10^5 days at 350 cm in the sulfate-depleted zone (Fig. S2, A). The

Table 2
Geochemical characterization and methanogenic activities in the Western Mediterranean Sea.

	GeoB17306		GeoB17308		GeoB17314
	SRZ	SDZ	SRZ	SDZ	SRZ
Methane (mM)	0.04 ± 0.01	3.5 ± 1.3	0.04 ± 0.12	1.3 ± 0.9	$6 \times 10^{-4} \pm 5 \times 10^{-4}$
Sulfate (mM)	16.6 ± 12.9	0.6 ± 0.4	14.7 ± 7.6	0.5 ± 0.5	30.5 ± 0.6
TOC (%)	0.9 ± 0.2	1.1 ± 0.3	0.5 ± 0.1	0.5 ± 0.02	0.2 ± 0.09
δ^{13}C-TOC (‰)	-27.1 ± 0.1	-26.5 ± 0.5	-25.1 ± 0.2	-25.2 ± 0.2	-23.3 ± 0.4
TOC accumulation rate (g C m^{-2} y^{-1})	1362 ± 290	1667 ± 473	17.5 ± 3.2	17.5 ± 0.9	–
DIC (mM)	18.2 ± 12.4	26.7 ± 4.2	5.0 ± 1.4	2.0 ± 0.9	2.2 ± 0.5
Acetate (μM)	3.7 ± 0.5	3.6 ± 1.8	3.2 ± 0.4	5.2 ± 0.05	2.5 ± 1.4
Methanol (μM)	0.9 ± 0.4	0.5 ± 0.4	0.2 ± 0.1	0.1 ± 0.04	0.7 ± 0.8
CO_2 turnover time (d)	$1.3 \times 10^6 \pm 3.8 \times 10^5$	$1.1 \times 10^5 \pm 6.1 \times 10^4$	$8.7 \times 10^6 \pm 9.1 \times 10^6$	$3.7 \times 10^6 \pm 3.2 \times 10^6$	$2.1 \times 10^6 \pm 2.4 \times 10^6$
Acetate turnover time (d)	$3.5 \times 10^6 \pm 2.1 \times 10^5$	53.8 ± 32.4	$1.0 \times 10^5 \pm 9.7 \times 10^4$	$2.3 \times 10^5 \pm 6.5 \times 10^4$	$1.2 \times 10^5 \pm 5.8 \times 10^4$
Methanol turnover time (d)	50.1 ± 12.6	45.6 ± 14.3	$5.7 \times 10^3 \pm 7.3 \times 10^3$	$6.6 \times 10^4 \pm 5.2 \times 10^4$	48.2 ± 27.3
Methylamine turnover time (d)	25.8 ± 3.5	46.6 ± 27.8	$1.0 \times 10^4 \pm 2.1 \times 10^4$	$2.6 \times 10^5 \pm 3.2 \times 10^5$	23.9 ± 6.65
H_2/CO_2 MOG (nmol cm^{-3} d^{-1})	0.01 ± 0.01	0.8 ± 0.6	$5.0 \times 10^{-3} \pm 7.1 \times 10^{-3}$	$9.7 \times 10^{-4} \pm 4.1 \times 10^{-4}$	$2.3 \times 10^{-3} \pm 1.7 \times 10^{-3}$
Acetate MOG (nmol cm^{-3} d^{-1})	$1.6 \times 10^{-4} \pm 1.0 \times 10^{-4}$	0.1 ± 0.1	$1.4 \times 10^{-4} \pm 1.7 \times 10^{-4}$	$3.0 \times 10^{-5} \pm 1.3 \times 10^{-5}$	$2.5 \times 10^{-5} \pm 2.3 \times 10^{-5}$
Methanol MOG (nmol cm^{-3} d^{-1})	0.02 ± 0.01	0.01 ± 0.01	$2.0 \times 10^{-3} \pm 1.9 \times 10^{-3}$	$2.8 \times 10^{-6} \pm 2.6 \times 10^{-6}$	0.02 ± 0.01
Total MOG rate (nmol cm^{-3} d^{-1})	0.04 ± 0.003	0.9 ± 0.6	$7.1 \times 10^{-3} \pm 9.2 \times 10^{-3}$	$1.0 \times 10^{-3} \pm 0.4 \times 10^{-3}$	0.02 ± 0.01

MOG: methanogenesis; SRZ: sulfate reduction zone (GeoB17306: 0–80 cm; GeoB17308: 0–270 cm; GeoB17314: 0–40 cm); SDZ: sulfate depleted zone (GeoB17306: 100–520 cm; GeoB17308: 290–400 cm). Values are mean (the average of total measured samples from SRZ or SDZ) ± S.D. TOC accumulation rates were calculated based on a density of 2.63 g cm^{-3} for dry sediment (Fagervold et al., 2014) and an average porosity of 0.6, and the rates were not calculated at GeoB17314 as the sedimentation rate was not available. MOG rates and turnover time were calculated based on Eqs. (1) and (2), respectively.

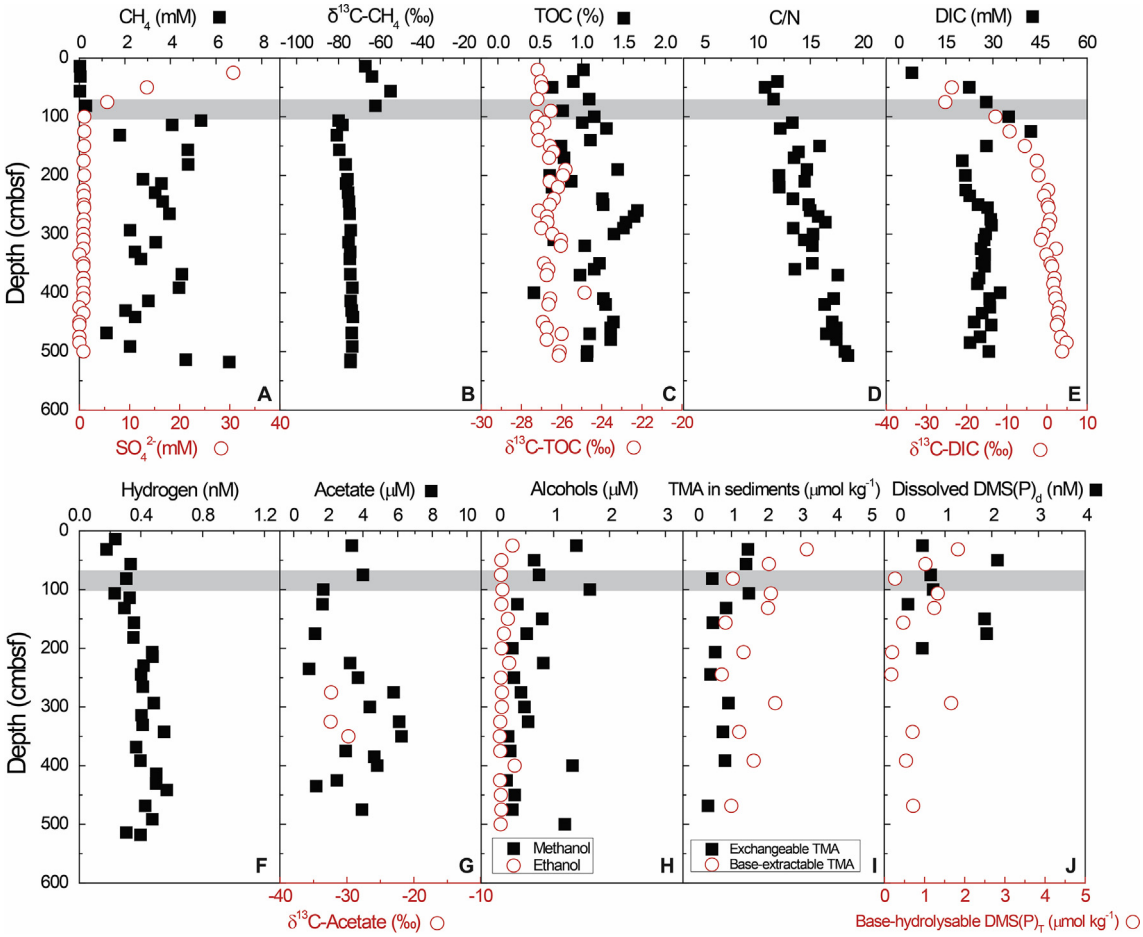

Fig. 2. Site GeoB17306: depth profiles of methane and sulfate (A), $\delta^{13}C$ of methane (B), TOC and $\delta^{13}C$ of TOC (C), C/N ratio (D), DIC and $\delta^{13}C$ of DIC (E), hydrogen (F) acetate and $\delta^{13}C$ of acetate (G), methanol and ethanol (H), exchangeable TMA and base-extractable TMA (I) and dissolved DMS(P)d and base-hydrolysable $DMS(P)_T$ (J) in pore waters and sediment. Note that exchangeable TMA, base-extractable TMA and base-hydrolysable $DMS(P)_T$ was expressed as μmol per kg wet sediment. SMTZ was marked with gray bars.

fastest turnover for acetate was observed at 75 cm (6.7×10^3 days) (Fig. S2, B); the turnover rate of acetate decreased by a factor of ten in the deeper sediment. Methanol and methylamine displayed a parallel trend with increasing turnover time with increasing depth. The most rapid turnover of methanol and methylamine was observed at 25 cm, with turnover times of 25 days and 29 days, respectively. The turnover time of these methylated substrates increased markedly with depth, and reached the maximum of 7.4×10^4 and 1.1×10^5 days at 350 cm (Fig. S2, C and D). Compared to GeoB17306, methanogenesis rates from bicarbonate, acetate and methanol were much lower. Relatively high activities were observed in the upper 75 cm for all amended substrates, and then the methanogenic rates generally decreased with increasing depth (Fig. 6).

In the surface sediment of GeoB17314, the average turnover time of methanol and methylamine was 46 days and 24 days, respectively, about ~3–5 orders of magnitude faster than bicarbonate (2.0×10^6 days) or acetate (1.1×10^5 days) (Fig. S3). Correspondingly, the highest methanogenesis rates were supported by methanol (0.03 nmol cm^{-3} d^{-1}) at 2 cm, about 30 times higher than hydrogenotrophic methanogenesis. Acetoclastic methanogenesis was detectable but at extremely low rates (~5×10^{-5} nmol cm^{-3} d^{-1}) (Fig. 7). The methane production rate from bicarbonate and acetate generally decreased with depth, while the opposite trend was observed for methanol-based methanogenesis.

3.4. Diversity of methanogenic Archaea

Diverse methanogen communities were detected with *mcrA* genes analysis at GeoB17306 and GeoB17308, and specified at least on the order level, or the genus and species level whenever possible. In the sulfate reduction zone of GeoB17306 (20–45 cm), sequences were exclusively affiliated within the orders *Methanomicrobiales* (43%) and *Methanosarcinales* (57%). Specifically, the clone library sequence assemblages contained genera or species related to *Methanoplanus limicola*, *Methanolobus bombayensis*, *Methanosarcina mazei* and *Methanococcoides* spp. (Fig. 8). At SMTZ (75–90 cm), sequences closely related to ANME-2a (i.e., ANaerobic MEthanotroph) comprised 55% of the retrieved sequences. The majority of methanogens belonged to the *Methanomicrobiales* (38%), and a few sequences were affiliated with the

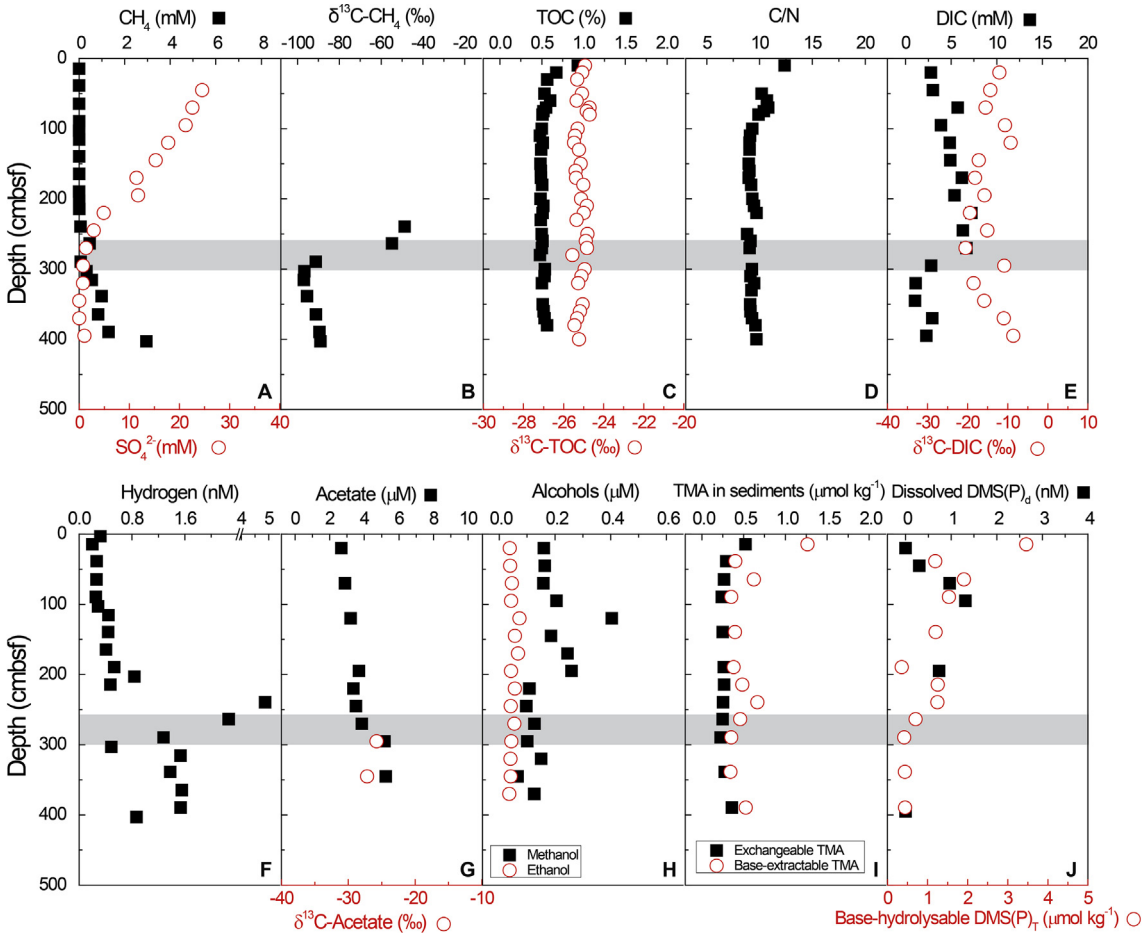

Fig. 3. Site GeoB17308: depth profiles of methane and sulfate (A), $\delta^{13}C$ of methane (B), TOC and $\delta^{13}C$ of TOC (C), C/N ratio (D), DIC and $\delta^{13}C$ of DIC (E), hydrogen (F) acetate and $\delta^{13}C$ of acetate (G), methanol and ethanol (H), exchangeable TMA and base-extractable TMA (I) and dissolved DMS(P)d and base-hydrolysable $DMS(P)_T$ (J) in pore waters and sediment. SMTZ was marked with gray bars.

Methanosarcinales (e.g., *Methanosarcina*) and *Methanomassiliicoccales* (Fig. 8). In the deeper sediment between 379 cm and 395 cm, members of *Methanomicrobiales* still dominated the methanogen communities (48%). Within the *Methanosarcinales*, sequences closely related to *Methanosarcina mazei* (14%) and other species of the genus *Methanosarcina* (9%) were more abundant in relative proportion than in the upper sediment (Fig. 8). At GeoB17308, the amplification of *mcrA* gene was only successful above SMTZ between 225 and 240 cm, probably due to the low abundance of methanogens at this site. Compared to GeoB17306, fewer sequences were recovered while the methanogen communities were more diverse, with additional genera present from the orders *Methanocellales* and *Methanobacteriales*. Sequences related to *Methanomicrobiales*, *Methanocellales* and *Methanosarcinales* accounted for 33%, 48%, and 26% of the assemblages, respectively (Fig. 8).

4. DISCUSSION

Geochemical analyses of methane and potential precursors, ^{14}C-based methanogenesis rate measurements and *mcrA* gene analysis revealed active methane production in surface and subsurface sediments of the Western Mediterranean Sea. At the selected sites with different geochemical settings and terrestrial organic matter input, methane production rates from various substrates differed distinctly. In particular, we found that methylotrophic methanogenesis occurred throughout the sediment cores and constituted the dominant methanogenic pathway in the sulfate reduction zone. These findings allow us to explore the relationships between depositional settings, substrate pools, and methanogenesis rates, the linkage between methanogenic substrates, pathway and community, and the coupling of methanogenesis and AOM in the sulfate reduction zone, which will be elaborated below.

4.1. The occurrence of methane and potential precursors

In the two deep gravity cores, methane occurred with low but detectable concentrations within the sulfate reduction zone, and accumulated with high abundance in the sulfate-depleted sediments (Table 2). The differing degrees of ^{13}C depletion in methane in the sulfate-bearing zone (e.g., $\delta^{13}C$ is between −55‰ and −67‰ at GeoB17306) vs. the sulfate-depleted zone (e.g., $\delta^{13}C$ is between −73‰

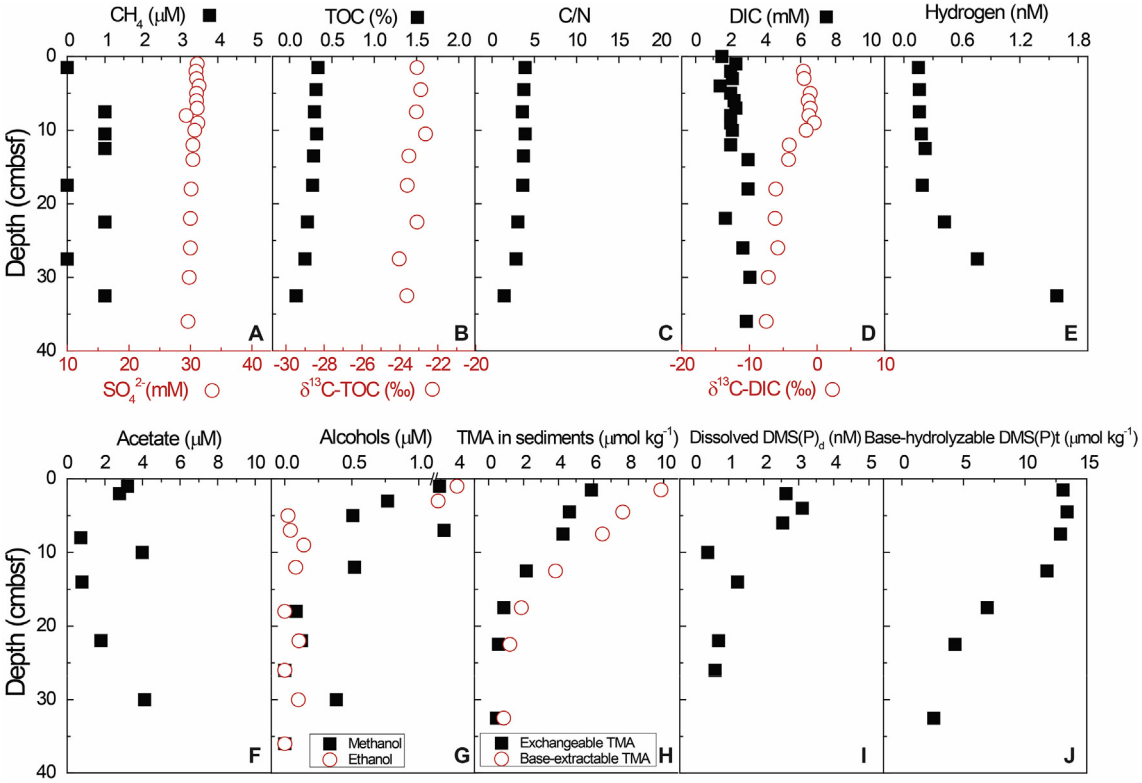

Fig. 4. Site GeoB17314: depth profiles of methane and sulfate (A), TOC and $\delta^{13}C$ of TOC (B), C/N ratio (C), DIC and $\delta^{13}C$ of DIC (D), hydrogen (E), acetate (F), methanol and ethanol (G), exchangeable TMA and base-extractable TMA (H), dissolved $DMS(P)_d$ (I) and base-hydrolysable $DMS(P)_T$ (J) in pore waters and sediment.

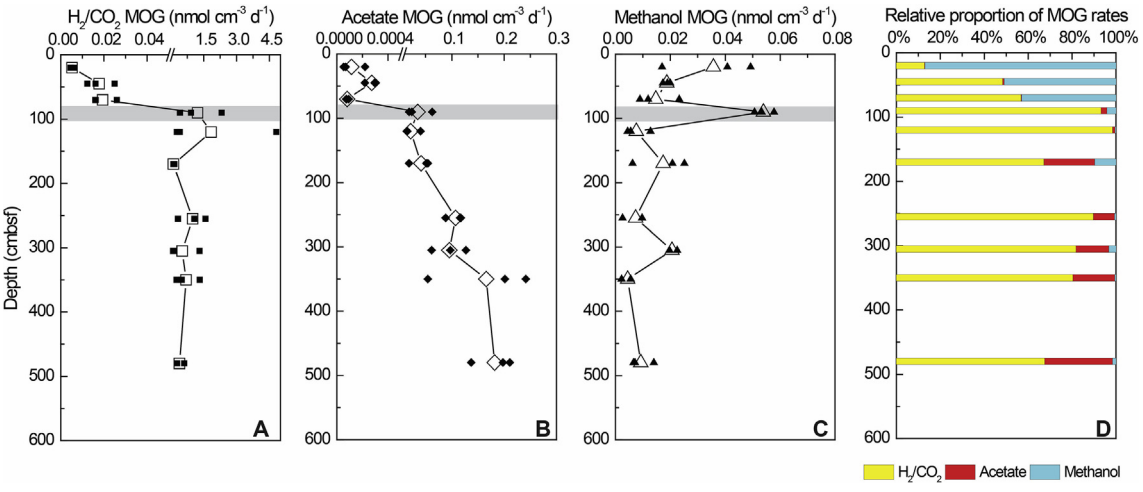

Fig. 5. Site GeoB17306: depth profiles of methanogenesis (MOG) rate from H_2/CO_2 (A), acetate (B) and methanol (C), and the relative proportion of MOG rate from different substrates (D). SMTZ was marked with gray bars. Triplicates (smaller solid symbols) and mean (larger open symbols with solid line) were shown for MOG rate. Note the break of the scale for H_2/CO_2 and acetate MOG, and some symbols were not visible either due to the overlap of the duplicates or the hiddenness by the scale break.

and −88‰ at GeoB17306) suggested the operation of different modes of methane turnover in these zones. This isotopic range as a whole is consistent with biological *in situ* production of methane throughout the sampled section at both sites (e.g., Whiticar, 1999). The relative ^{13}C-enrichment in the sulfate-bearing zone most likely results from a different mode of methanogenesis combined with the sulfate-dependent methane oxidation; this process is consistent with the presence of ANMEs (Fig. 8, see discussion below).

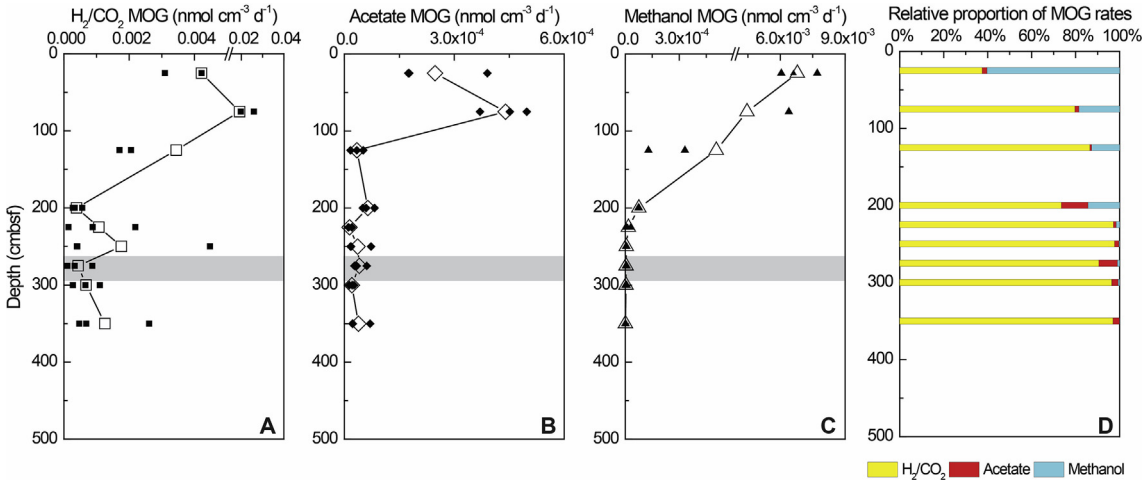

Fig. 6. Site GeoB17308: depth profiles of methanogenesis (MOG) rate from H_2/CO_2 (A), acetate (B) and methanol (C), and the relative proportion of MOG rate from different substrates (D). SMTZ was marked with gray bars. Triplicates (smaller symbols) and mean (larger symbols with solid line) were shown for methanogenesis rate. Note the break of the scale for H_2/CO_2 and methanol MOG, and some symbols were not visible either due to the overlap of the duplicates or the hiddenness by the scale break.

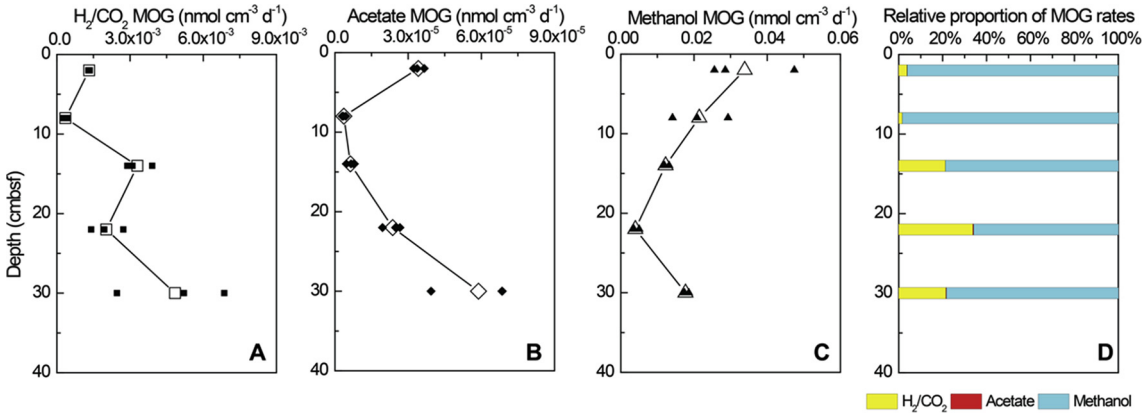

Fig. 7. Site GeoB17314: depth profiles of methanogenesis (MOG) rate from H_2/CO_2 (A), acetate (B) and methanol (C), and the relative proportion of MOG rate from different substrates (D). Triplicates (smaller solid symbols) and mean (larger open symbols with solid line) were shown for MOG rate. Some symbols were not visible due to the overlap of the duplicates.

To decipher the potential sources of methane, we first investigated the abundance of low molecular weight methanogenic compounds (e.g., acetate, methanol, methylated amine and sulfide), which are important intermediates during organic matter degradation and their distribution might be influenced by different depositional settings and sources of organic matter.

Acetate concentrations were in the low micromolar range at all three sites, similar to values reported for other shallow coastal and deep-sea marine sediments (D'Hondt et al., 2003; Jørgensen and Parkes, 2010; Ijiri et al., 2012; Glombitza et al., 2015). The similarity of $\delta^{13}C$ values of acetate and TOC indicated that acetate was predominantly generated from the degradation of organic matter (cf. Heuer et al., 2009). The lack of an obvious proportionality between TOC and acetate concentration suggests that the acetate pool size might be controlled by biological processes rather than the size of the potential precursor pool, in analogy to hydrogen in marine sediments (e.g., Hoehler et al., 1998). Once produced, acetate or hydrogen could be used by multiple microorganisms, and the microbial consumption would result in the concentrations of those intermediates maintained at some threshold level (Glombitza et al., 2015).

The important methylated substrate methanol was detected at low concentration (<3 μM) in the sedimentary pore waters (Fig. 2; 3; 4H). Methanol can be derived from the presence of terrigenous lignin and pectin in marine sediment (Donnelly and Dagley, 1980; Schink and Zeikus, 1980), and the abundance and decomposition of fresh organic matter can contribute to the accumulation of methanol in surface sediments (e.g., GeoB17306) (Zhuang et al., 2014). Hence, the higher abundance of methanol at GeoB17306 compared to GeoB17308 (Table 2) agrees well with the decreasing input of terrestrial organic matter from the prodelta to the shelf.

Due to the strong adsorption on the sediments (Wang and Lee, 1990, 1993; Fitzsimons et al., 2006; Zhuang et al., 2017), TMA was barely detectable at most depths

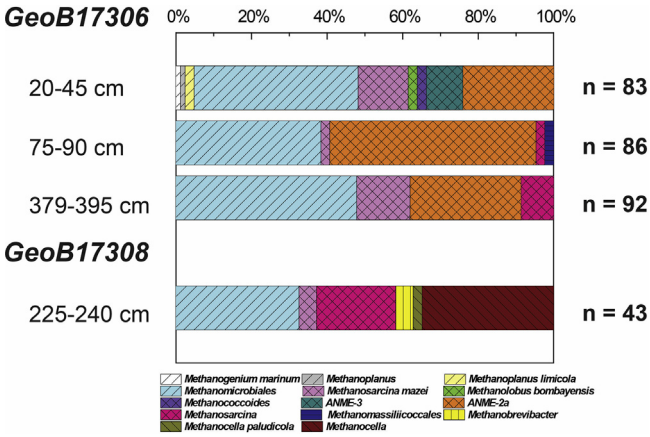

Fig. 8. Depth profile of relative abundance of methanogen populations at Site GeoB17306 and GeoB17308 based on *mcrA* genes clone libraries. Genera and species belonging to different orders (see Table S1) were marked with different patterns. The numbers (*n*) represented the total sequences of methanogens recovered from each depth.

in the pore waters (<20 nM) at all sites, whereas the pool sizes in the sediment solid phase were relatively large. The existence of abundant exchangeable TMA (extracted with LiCl to compete for adsorption) indicated a substantial pool of potentially bioavailable TMA, which could be utilized for microbial processes in sediments (Wang and Lee, 1993). Likewise, the concentrations of base-hydrolysable DMSP in the sediments were about three orders of magnitude higher than the combined pool of dissolved DMS and DMSP in the pore water (<3 nM). Methylated amines and sulfur compounds could be derived from a number of potential precursors (e.g., choline, glycine betaine, DMSP) that are largely formed by phytoplankton and act as osmolytes (Keller et al., 1999; Belviso et al., 2006; Zhuang et al., 2011). Upon deposition at the seafloor, these precursors can be degraded to TMA and DMS, which constitute highly energetic substrates for methanogenesis as well as non-methanogenic processes (Oremland and Polcin, 1982; King, 1984; Kiene et al., 1986; van der Maarel and Hansen, 1997; Zhuang et al., 2017). In this regard, the higher concentration of TMA at Site GeoB17306 than at Site GeoB17308 could be possibly explained by the higher marine primary production that was stimulated by considerable riverine input of nutrients. The larger pools of TMA and DMS(P) at Site GeoB17314 are consistent with the higher proportion of marine organic matter, as reflected from the less negative isotopic values of TOC.

Collectively, these data suggest that the abundance of methane precursors could be related to the sources (terrestrial vs marine) and quantities of organic matter for each of the three sites. The differences in geochemistry, organic matter and substrate pools could further influence methanogenic rates and pathways, which will be discussed below.

4.2. The influence of geochemistry and substrates on methanogenic activity

Rate measurements demonstrated the influence of environmental factors on the potential for methanogenic activity: for all amended ^{14}C labeled substrates, rates of methanogenesis varied with depths and sites. At the prodelta site GeoB17306, methanogenesis rates from bicarbonate and acetate were much lower in the sulfate reduction zone than in the sulfate-depleted sediment (Table 2). This is not surprising as sulfate reducers outcompeted methanogens for hydrogen and acetate. In contrast, high methanogenesis rates from methanol and rapid turnover of methylamine in the sulfate reduction zone confirmed that methylated compounds were less competitive methanogenic substrates and also indicated that methylotrophic methanogenesis was the dominant methanogenic pathway in the presence of high levels of sulfate. After sulfate was exhausted, acetate and hydrogen were available for methanogens. As a result, hydrogenotrophic and acetoclastic methanogenesis rates increased and methane was largely produced from H_2/CO_2 or to a lesser extent acetate. While the presence of sulfate inhibited the methanogenic activity at the prodelta site, the shelf site showed higher hydrogenotrophic and acetoclastic rates in the sulfate zone compared to the sulfate-depleted zone below (Table 2). Those differences between sites suggested sulfate was not the sole factor controlling the production of methane.

Because of the different sedimentation and TOC accumulation rates in the prodelta and on the shelf, organic matter age might critically impact the methanogenic capacity at Sites GeoB17306 and 17308, respectively. Young sediments contain fresh organic matter, and the presence of labile organic matter is advantageous for the degradation of organic carbon and the release of substrates (Schmidt et al., 2017), further facilitating the production of methane. With increasing age, organic matter becomes less reactive and therefore substrates are less available in greater sediment depth. This concept is supported by the recent study of Peruvian margin sediment, where the availability of labile organic matter has been found to be the dominant factor controlling surface methanogenesis (Maltby et al., 2016). In the prodelta, considerable riverine inputs and high sedimentation rate (i.e., 35 cm/a) lead to the delivery of fresh material to the seafloor, thus influence the quantity, quality and mineralization of the organic matter. The

average TOC accumulation rate was 1622 g C m^{-2} y^{-1} at Site GeoB17306, about 100 times of that at Site GeoB17308 (17.5 g C m^{-2} y^{-1}) (Table 2). Correspondingly, the ages of the organic matter differed distinctly. The estimated age for the deepest sample taken from Site GeoB17306 (516 cm) was only around 15 years based on the accumulation rates of approximately 35 cm/a, whereas the 405 cm deep sediment at Site GeoB17308 had a maximum age of 620 years (0.65 cm/a). Much lower methanogenic activities were detected at the shelf site GeoB17308, and methanogenesis rates from H_2/CO_2 below SMTZ were lower by 2–3 orders of magnitude than those at the prodelta site GeoB17306 (Table 2). Similarly, acetoclastic methanogenesis rates were extremely low throughout core GeoB17308 ($<4 \times 10^{-4}$ nmol cm^{-3} d^{-1}), but reached up to 0.2 nmol cm^{-3} d^{-1} in the sulfate-depleted sediment at GeoB17306. In the same fashion, the decrease of other substrate pools, such as methanol, also lowered the methylotrophic methanogenesis rates in shelf sediments compared to prodelta sediments. Although we could not estimate the organic matter age at Site GeoB17314 off the Moulouya River due to the lack of data for sedimentation rates, the lower methanogenesis rates from H_2/CO_2 and acetate at GeoB17314 than those rates in the sulfate reduction zone of GeoB17306 and GeoB17308, was consistent with the lower TOC content observed at this site. Taken all those observations together, we conclude that the presence of sulfate, and the quantity and age of organic matter are the driving factors for variations in methanogenic activities between sites and over depth.

4.3. The linkage between the methanogenic substrate, pathway and diversity

To better understand the methanogenic process, we analyzed the functional gene for the alpha subunit of methyl coenzyme M reductase (*mcrA*), a key enzyme of methanogenesis and anaerobic methane oxidation (Friedrich, 2005). The identification of the methanogenic populations allows us to link the taxonomic information to the substrate pools and methanogenic pathways.

In the sulfate reduction zone, the availability and rapid turnover of methylated compounds led to considerable methane production via methylotrophic methanogenesis, and methanol accounted for 43–87% of total measured methane production rate (Fig. 6D). Accordingly, methylotrophic methanogens were detected between 25 cm and 40 cm. The genus of *Methanococcoides* and the species of *Methanolobus bombayensis* are obligate methylotrophic methanogens, and they grow exclusively on methylated compounds (Table S1). A number of sequences were related to *Methanosarcina mazei*, which can metabolize the major substrates from three methanogenic pathways. Due to the incomplete inhibition from the sulfate reducers, hydrogenotrophic methanogenesis occurred and could contribute to 13–57% of the methane production in the sulfate-reducing sediments. Correspondingly, abundant hydrogenotrophic methanogens within the order of *Methanomicrobiales* were also found at this horizon.

Between 75 cm and 90 cm, the majority of detected *mcrA* genes belonged to hydrogenotrophic *Methanomicrobiales*. Interestingly, sequences of the recently proposed seventh order of methanogens *Methanomassiliicoccales* (Iino et al., 2013) were detected at this depth. The presence of methanol provided energetic substrate for those methanogens as cultured or enriched members from this order could only metabolize methanol with hydrogen to produce methane (Dridi et al., 2012). The sequence-based detection of *Methanomassiliicoccales* in marine sediments, together with the discovery of their unique membrane lipids (cf. Becker et al., 2016) in estuarine and deep subseafloor sediments (Zhu et al., 2014; Meador et al., 2015), indicates that this new order is more widespread in natural environment than previously thought.

In the sulfate-depleted sediment, high hydrogenotrophic methanogenesis rates accounted for 67–98% of the total methane production (Fig. 6D), in accordance with the predominance of *Methanomicrobiales* in retrieved sequences. Acetoclastic methanogenesis was also active, and its contribution to methane production increased to a larger proportion, e.g., a maximum of 31% at 480 cm. Consistently, *Methanosarcinales* were slightly more abundant in relative proportion than in the sulfate reduction zone, and the increasing abundance of *Methanosarcina* suggested that acetate might be the major substrate for this versatile genus. In contrast, the role of methylotrophic methanogenesis was significantly reduced compared to the sulfate reduction zone (e.g., 43–87% vs. <3%), and no obligate methylotrophic methanogen was observed at this depth.

At Site GeoB17308, the *mcrA* gene could be only amplified between 225 and 240 cm, presumably due to the lower availability of substrates and lower microbial activity at this site. Still, methylated compounds were important methanogenic substrates in the upper sulfate reduction zone (fueling up to 60% of methane production), while the contribution of methanol to methane production decreased due to the reduced availability of substrates. With the depletion of sulfate, methane was predominantly generated from H_2/CO_2 (e.g., ~97%). A minor fraction of methane was produced from acetate in both the sulfate-reducing and sulfate-depleted zones (<3%), indicating the quantitative insignificance of acetoclastic methanogenesis at this site. Consistent with the predominance of hydrogenotrophic methanogenesis, all the methanogenic taxa detected between 225 and 240 cm belonged consistently to genera and families with cultured representatives utilizing hydrogen and bicarbonate to produce methane. Overall, the metabolisms of different substrates and the relative importance of individual pathways could be linked to the diverse and dynamic assemblage of methanogen communities at different zonations.

4.4. Methane cycling and the importance of methylotrophic methanogenesis in surface sediment

Due to the closeness to the sediment-water interface, microbial methanogenesis in surface sediment might be a potential source for methane emission to the water column (Maltby et al., 2016). To further illustrate the mechanism and magnitude of surface methanogenesis, we carried out

high-resolution sampling of sulfate-rich surface sediments for rate measurements at Site GeoB17314. Notably, highest methanogenesis rates were induced by methanol (~0.03 nmol cm^{-3} d^{-1}) at 2 cm, and methanol-based methanogenesis accounted for ~66–98% of total methane production in the upper 30 cm sediment, confirming the particular importance of methylotrophic methanogenesis in the sulfate-bearing sediment. This is consistent with the finding from a recent study, which identified that a benthic methane source from methylotrophic methanogenesis resulted in the methane flux to the overlying anoxic water in the Eastern Tropical North Pacific oxygen minimum zone (Chronopoulou et al., 2017). The production of methane from methanol reflects potential rates only due to the additional substrate added by the tracer. However, the production and ubiquity of various methylated compounds in the pristine sediments clearly point to the potential for methylotrophic methanogenesis occurring in natural environments, as well. For example, the presence of methanol in the pore water despite the high methanol-based methanogenesis suggested persistent methanol production occurred and balanced the rapid consumption of methanol. This conclusion is also supported by a recent study (Yanagawa et al., 2016), which demonstrated that high methanol production and consumption rates were balanced in the anoxic marine sediments.

Despite of the high methanogenesis rate, methane could be microbially consumed before escaping the sediment. Indeed, the enrichment of ^{13}C in methane as well as the lack of methane accumulation, suggested that AOM potentially occurred in the sulfate reduction zone of Site GeoB17306. The high frequency of detecting ANME-2 and ANME-3 sequences is strongly suggestive of the activity of AOM in the sulfate-reducing sediment. Hence, AOM could act as an effective barrier to methane release from the surface sediments through a close coupling to methylotrophic methanogenesis in the sulfate reduction zone. A potential efflux of methane from the sediment needs to be constrained with more precise profiling of methane at the sediment-water interfaces and surrounding bottom water. Furthermore, due to the presence of abundant methylated compounds such as TMA and DMSP in the seawater, methylotrophic methanogenesis might be ubiquitous in anoxic microniches of the oceanic water column (Damm et al., 2008).

5. CONCLUSIONS

We conducted integrated biogeochemical investigations on methanogenic substrates, activity and diversity to constrain different factors that control the microbial production of methane and further quantitatively estimate the relative importance of different methanogenic pathways in marine sediments of the Western Mediterranean Sea. We found that methylotrophic methanogenesis played an essential role in the sulfate-reducing sediments and contributed up to 98% of the total methane production in the surface sediment. Hydrogenotrophic methanogenesis dominated the methane production in the absence of sulfate, and acetate could enhance methane production in organic-rich sediment. Our findings suggest that not only the presence of sulfate but also the quantity and age of organic matter govern the type and extend of methanogenic activity in marine sediments, while information on the abundance of methanogenic substrates is not sufficient to predict the methane production potential. The evidence for methylotrophic methanogenesis in surface sediments has further implications; methane produced by this pathway above the SMTZ could possibly drive AOM in surficial sediments, while the release of this methane into the water column could potentially influence the benthic methane budget in the ocean.

ACKNOWLEDGEMENTS

We acknowledge the captain, crew as well as the scientists of R/V Poseidon cruise POS450 for their kind assistance during sampling. We are grateful for J. Arndt for the support of DIC stable carbon isotopic analysis and M. Bowles for the valuable comments on the manuscript. We thank associate editor Ed Hornibrook and two anonymous reviewers for providing comments that improved an earlier version of this manuscript. The study was funded by the European Research Council under the European Union's (EU) Seventh Framework Programme, "Ideas" Specific Programme, ERC Grant Agreement 247153 [Advanced Grant DARCLIFE (to K.-U. H.)] and by the Deutsche Forschungsgemeinschaft (DFG) through the DFG-Research Center and Excellence Cluster 'The Ocean in the Earth System'. Rate measurements were supported by a grant from the US National Science Foundation's Emerging Frontiers program (award 0801741 to S. B. Joye). G.-C. Zhuang was jointly sponsored by the Chinese Scholarship Council (CSC) and the Bremen International Graduate School for Marine Sciences (GLOMAR). The dataset has been deposited in the PANGAEA database at https://www.pangaea.de (doi: 10.1594/PANGAEA.883599).

APPENDIX A. SUPPLEMENTARY MATERIAL

Supplementary data associated with this article can be found, in the online version, at https://doi.org/10.1016/j.gca.2017.12.024.

REFERENCES

Altschul S. F., Gish W., Miller W., Myers E. W. and Lipman D. J. (1990) Basic local alignment search tool. *J. Mol. Biol.* **215**, 403–410.

Becker K. W., Elling F. J., Yoshinaga M. Y., Söllinger A., Urich T. and Hinrichs K.-U. (2016) Unusual butane-and pentanetriol-based tetraether lipids in *Methanomassiliicoccus luminyensis*, a representative of the seventh order of methanogens. *Appl. Environ. Microbiol.* **82**, 4505–4516.

Belviso S., Thouzeau G., Schmidt S., Reigstad M., Wassmann P., Arashkevich E. and Stefels J. (2006) Significance of vertical flux as a sink for surface water DMSP and as a source for the sediment surface in coastal zones of northern Europe. *Estuar. Coast. Shelf Sci.* **68**, 473–488.

Bowles M. W., Samarkin V. A. and Joye S. B. (2011) Improved measurement of microbial activity in deep-sea sediments at in situ pressure and methane concentration. *Limnol. Oceanogr.-Methods* **9**, 499–506.

Canals M., Puig P., de Madron X. D., Heussner S., Palanques A. and Fabres J. (2006) Flushing submarine canyons. *Nature* **444**, 354–357.

Chronopoulou P.-M., Shelley F., Pritchard W. J., Maanoja S. T. and Trimmer M. (2017) Origin and fate of methane in the Eastern Tropical North Pacific oxygen minimum zone. *ISME J.* **11**, 1386–1399.

Chuang P. C., Young M. B., Dale A. W., Miller L. G., Herrera-Silveira J. A. and Paytan A. (2016) Methane and sulfate dynamics in sediments from mangrove-dominated tropical coastal lagoons, Yucatán, Mexico. *Biogeosciences* **13**, 2981–3001.

D'Hondt S. L., Jørgensen B. B., and Miller D. J., et al. (2003) Proc. ODP, Init. Repts., 201: College Station, TX (Ocean Drilling Program). http://doi:10.2973/odp.proc.ir.201.2003.

D'Hondt S. L., Jørgensen B. B. and Miller D. J., et al. (2004) Distributions of microbial activities in deep subseafloor sediments. *Science* **306**, 2216–2221.

Damm E., Kiene R. P., Schwarz J., Falck E. and Dieckmann G. (2008) Methane cycling in Arctic shelf water and its relationship with phytoplankton biomass and DMSP. *Mar. Chem.* **109**, 45–59.

Donnelly M. I. and Dagley S. (1980) Production of methanol from aromatic acids by Pseudomonas putida. *J. Bacteriol.* **142**, 916–924.

Dridi B., Fardeau M.-L., Ollivier B., Raoult D. and Drancourt M. (2012) *Methanomassiliicoccus luminyensis* gen. nov., sp. nov., a methanogenic archaeon isolated from human faeces. *Int. J. Syst. Evol. Microbiol.* **62**, 1902–1907.

Ertefai T. F., Heuer V. B., Prieto-Mollar X., Vogt C., Sylva S. P., Seewald J. and Hinrichs K.-U. (2010) The biogeochemistry of sorbed methane in marine sediments. *Geochim. Cosmochim. Acta* **74**, 6033–6048.

Evans P. N., Parks D. H., Chadwick G. L., Robbins S. J., Orphan V. J., Golding S. D. and Tyson G. W. (2015) Methane metabolism in the archaeal phylum Bathyarchaeota revealed by genome-centric metagenomics. *Science* **350**, 434–438.

Fagervold S. K., Bourgeois S., Pruski A. M., Charles F., Kerhervé P., Vétion G. and Galand P. E. (2014) River organic matter shapes microbial communities in the sediment of the Rhône prodelta. *ISME J.* **8**, 2327–2338.

Fitzsimons M. F., Millward G. E., Revitt D. M. and Dawit M. D. (2006) Desorption kinetics of ammonium and methylamines from estuarine sediments: consequences for the cycling of nitrogen. *Mar. Chem.* **101**, 12–26.

Friedrich M. W. (2005) Methyl-coenzyme M reductase genes: unique functional markers for methanogenic and anaerobic methane-oxidizing Archaea. *Meth. Enzymol.* **26**, 428–442.

Glombitza C., Jaussi M., Røy H., Seidenkrantz M.-S., Lomstein B. A. and Jørgensen B. B. (2015) Formate, acetate, and propionate as substrates for sulfate reduction in sub-arctic sediments of Southwest Greenland. *Front. Microbiol.* **6**. https://doi.org/10.3389/fmicb.2015.00846.

Goldhammer T., Brunner B., Bernasconi S. M., Ferdelman T. G. and Zabel M. (2011) Phosphate oxygen isotopes: Insights into sedimentary phosphorus cycling from the Benguela upwelling system. *Geochim. Cosmochim. Acta* **75**, 3741–3756.

Hales B. A., Edwards C., Ritchie D. A., Hall G., Pickup R. W. and Saunders J. R. (1996) Isolation and identification of methanogen-specific DNA from blanket bog peat by PCR amplification and sequence analysis. *Appl. Environ. Microbiol.* **62**, 668–675.

Heuer V. B., Aiello I. W., Elvert M., Goldenstein N., Goldhammer T., Könneke M., Liu X., Pape S., Schmidt F., Wendt J. and Zhuang G.-C. (2014) Report and preliminary results of R/V POSEIDON cruise POS450, DARCSEAS II-Deep subseafloor archaea in the Western Mediterranean Sea: Carbon cycle, life Strategies, and role in sedimentary ecosystems, Barcelona (Spain)-Malaga (Spain), April 2–13, 2013. Berichte, MARUM-Zentrum für Marine Umweltwissenschaften, Fachbereich Geowissenschaften, Universität Bremen, 305, 42 pages. Bremen. ISSN 2195-9633.

Heuer V. B., Elvert M., Tille S., Krummen M., Mollar X. P., Hmelo L. R. and Hinrichs K.-U. (2006) Online $\delta^{13}C$ analysis of volatile fatty acids in sediment/porewater systems by liquid chromatography-isotope ratio-mass spectrometry. *Limnol. Oceanogr.-Methods* **4**, 346–357.

Heuer V. B., Pohlman J. W., Torres M. E., Elvert M. and Hinrichs K.-U. (2009) The stable carbon isotope biogeochemistry of acetate and other dissolved carbon species in deep subseafloor sediments at the northern Cascadia Margin. *Geochim. Cosmochim. Acta* **73**, 3323–3336.

Heuer V. B., Krüger M., Elvert M. and Hinrichs K.-U. (2010) Experimental studies on the stable carbon isotope biogeochemistry of acetate in lake sediments. *Org. Geochem.* **41**, 22–30.

Hoehler T. M., Alperin M. J., Albert D. B. and Martens C. S. (1998) Thermodynamic control on hydrogen concentrations in anoxic sediments. *Geochim. Cosmochim. Acta* **62**, 1745–1756.

Iino T., Tamaki H., Tamazawa S., Ueno Y., Ohkuma M., Suzuki K.-I., Igarashi Y. and Haruta S. (2013) *Candidatus* Methanogranum caenicola: a novel methanogen from the anaerobic digested sludge, and proposal of *Methanomassiliicoccaceae* fam. nov. and *Methanomassiliicoccales* ord. nov., for a methanogenic lineage of the class *thermoplasmata*. *Microbes Environ.* **28**, 244–250.

Ijiri A., Harada N., Hirota A., Tsunogai U., Ogawa N. O., Itaki T., Khim B.-K. and Uchida M. (2012) Biogeochemical processes involving acetate in sub-seafloor sediments from the Bering Sea shelf break. *Org. Geochem.* **48**, 47–55.

Jørgensen B. B. and Parkes R. J. (2010) Role of sulfate reduction and methane production by organic carbon degradation in eutrophic fjord sediments (Limfjorden, Denmark). *Limnol. Oceanogr.* **55**, 1338–1352.

Keller M. D., Kiene R. P., Matrai P. A. and Bellows W. K. (1999) Production of glycine betaine and dimethylsulfoniopropionate in marine phytoplankton. I. Batch cultures. *Mar. Biol.* **135**, 237–248.

Kessler J. D., Reeburgh W. S., Valentine D. L., Kinnaman F. S., Peltzer E. T., Brewer P. G., Southon J. and Tyler S. C. (2008) A survey of methane isotope abundance (^{14}C, ^{13}C, ^{2}H) from five nearshore marine basins that reveals unusual radiocarbon levels in subsurface waters. *J. Geophys. Res.* **113**, C12021. https://doi.org/10.1029/2008JC004822.

Kiene R. P., Oremland R. S., Catena A., Miller L. G. and Capone D. G. (1986) Metabolism of reduced methylated sulfur compounds in anaerobic sediments and by a pure culture of an estuarine methanogen. *Appl. Environ. Microbiol.* **52**, 1037–1045.

King G. M., Klug M. J. and Lovley D. R. (1983) Metabolism of acetate, methanol, and methylated amines in intertidal sediments of lowes cove, Maine. *Appl. Environ. Microbiol.* **45**, 1848–1853.

King G. M. (1984) Utilization of hydrogen, acetate, and "non-competitive"; substrates by methanogenic bacteria in marine sediments. *Geomicrobiol. J.* **3**, 275–306.

King G. M. (1988) *Distribution and Metabolism of Quaternary Amines in Marine Sediments*. John Wiley and Sons, Chichester, United Kingdom.

Krzycki J. A., Kenealy W. R., DeNiro M. J. and Zeikus J. G. (1987) Stable carbon isotope fractionation by Methanosarcina barkeri during methanogenesis from acetate, methanol, or carbon dioxide-hydrogen. *Appl. Environ. Microbiol.* **53**, 2597–2599.

Larkin M. A., Blackshields G., Brown N., Chenna R., McGettigan P. A., McWilliam H., Valentin F., Wallace I. M., Wilm A., Lopez R., Thompson J. D., Gibson T. J. and Higgins D. G. (2007) Clustal W and Clustal X version 2.0. *Bioinformatics* **23**, 2947–2948.

Lee C. and Olson B. L. (1984) Dissolved, exchangeable and bound aliphatic amines in marine sediments: initial results. *Org. Geochem.* **6**, 259–263.

Lin Y.-S., Heuer V. B., Goldhammer T., Kellermann M. Y., Zabel M. and Hinrichs K.-U. (2012) Towards constraining H2 concentration in subseafloor sediment: a proposal for combined analysis by two distinct approaches. *Geochim. Cosmochim. Acta* **77**, 186–201.

Liu Y. and Whitman W. B. (2008) Metabolic, phylogenetic, and ecological diversity of the methanogenic archaea. *Ann. N. Y. Acad. Sci.* **1125**, 171–189.

Maltby J., Sommer S., Dale A. W. and Treude T. (2016) Microbial methanogenesis in the sulfate-reducing zone of surface sediments traversing the Peruvian margin. *Biogeosciences* **13**, 283–299.

Meador T. B., Bowles M., Lazar C. S., Zhu C., Teske A. and Hinrichs K.-U. (2015) The archaeal lipidome in estuarine sediment dominated by members of the Miscellaneous Crenarchaeotal Group. *Environ. Microbiol.* **17**, 2441–2458.

Milkov A. V. (2004) Global estimates of hydrate-bound gas in marine sediments: how much is really out there? *Earth-Sci. Rev.* **66**, 183–197.

Miralles J., Radakovitch O. and Aloisi J. C. (2005) 210Pb sedimentation rates from the Northwestern Mediterranean margin. *Mar. Geol.* **216**, 155–167.

Mitterer R. M., Malone M. J., Goodfriend G. A., Swart P. K., Wortmann U. G., Logan G. A., Feary D. A. and Hine A. C. (2001) Co-generation of hydrogen sulfide and methane in marine carbonate sediments. *Geophys. Res. Lett.* **28**, 3931–3934.

Oremland R. S. and Polcin S. (1982) Methanogenesis and sulfate reduction: competitive and noncompetitive substrates in estuarine sediments. *Appl. Environ. Microbiol.* **44**, 1270–1276.

Oremland R. S., Marsh L. M. and Polcin S. (1982) Methane production and simultaneous sulphate reduction in anoxic, salt marsh sediments. *Nature* **296**, 143–145.

Pante E. and Simon-Bouhet B. (2013) Marmap: a package for importing, plotting and analyzing bathymetric and topographic data in R. *PLoS ONE* **8**, 6–9.

Parkes R. J., Brock F., Banning N., Hornibrook E. R. C., Roussel E. G., Weightman A. J. and Fry J. C. (2012) Changes in methanogenic substrate utilization and communities with depth in a salt-marsh, creek sediment in southern England. *Estuar. Coast. Shelf Sci.* **96**, 170–178.

Schink B. and Zeikus J. G. (1980) Microbial methanol formation: a major end product of pectin metabolism. *Curr. Microbiol.* **4**, 387–389.

Schmidt F., Koch B. P., Goldhammer T., Elvert M., Witt M., Lin Y.-S., Wendt J., Zabel M., Heuer V. B. and Hinrichs K.-U. (2017) Unraveling signatures of biogeochemical processes and the depositional setting in the molecular composition of pore water DOM across different marine environments. *Geochim. Cosmochim. Acta* **207**, 57–80.

Seeberg-Elverfeldt J., Schlüter M., Feseker T. and Kölling M. (2005) Rhizon sampling of pore waters near the sediment/water interface of aquatic systems. *Limnol. Oceanogr.-Methods* **3**, 361–371.

Summons R. E., Franzmann P. D. and Nichols P. D. (1998) Carbon isotopic fractionation associated with methylotrophic methanogenesis. *Org. Geochem.* **28**, 465–475.

Tamura K., Dudley J., Nei M. and Kumar S. (2007) MEGA4: molecular evolutionary genetics analysis (MEGA) software version 4.0. *Mol. Biol. Evol.* **24**, 1596–1599.

Tesi T., Miserocchi S., Goñi M. A. and Langone L. (2007) Source, transport and fate of terrestrial organic carbon on the western Mediterranean Sea, Gulf of Lions, France. *Mar. Chem.* **105**, 101–117.

Valentine D. L. (2011) Emerging topics in marine methane biogeochemistry. *Annu. Rev. Mar. Sci.* **3**, 147–171.

van der Maarel M. J. E. C. and Hansen T. A. (1997) Dimethylsulfoniopropionate in anoxic intertidal sediments: a precursor of methanogenesis via dimethyl sulfide, methanethiol, and methiolpropionate. *Mar. Geol.* **137**, 5–12.

Vanwonterghem I., Evans P. N., Parks D. H., Jensen P. D., Woodcroft B. J., Hugenholtz P. and Tyson G. W. (2016) Methylotrophic methanogenesis discovered in the archaeal phylum Verstraetearchaeota. *Nat. Microbiol.* **1**, 16170. https://doi.org/10.1038/nmicrobiol.2016.170.

Wang X.-C. and Lee C. (1990) The distribution and adsorption behavior of aliphatic amines in marine and lacustrine sediments. *Geochim. Cosmochim. Acta* **54**, 2759–2774.

Wang X.-C. and Lee C. (1993) Adsorption and desorption of aliphatic amines, amino acids and acetate by clay minerals and marine sediments. *Mar. Chem.* **44**, 1–23.

Wang X.-C. and Lee C. (1994) Sources and distribution of aliphatic amines in salt marsh sediment. *Org. Geochem.* **22**, 1005–1021.

Whiticar M. J. (1999) Carbon and hydrogen isotope systematics of bacterial formation and oxidation of methane. *Chem. Geol.* **161**, 291–314.

Xie S., Lazar C. S., Lin Y.-S., Teske A. and Hinrichs K.-U. (2013) Ethane- and propane-producing potential and molecular characterization of an ethanogenic enrichment in an anoxic estuarine sediment. *Org. Geochem.* **59**, 37–48.

Yanagawa K., Tani A., Yamamoto N., Hachikubo A., Kano A., Matsumoto R. and Suzuki Y. (2016) Biogeochemical cycle of methanol in anoxic deep-sea sediments. *Microbes Environ.* **31**, 190–193.

Zhu C., Meador T. B., Dummann W. and Hinrichs K.-U. (2014) Identification of unusual butanetriol dialkyl glycerol tetraether and pentanetriol dialkyl glycerol tetraether lipids in marine sediments. *Rapid Commun. Mass Spectrom.* **28**, 332–338.

Zhuang G.-C., Elling F. J., Nigr L. M., Samarkin V., Joye S. B., Teske A. and Hinrichs K.-U. (2016) Multiple evidence for methylotrophic methanogenesis as the dominant methanogenic pathway in hypersaline sediments from the Orca Basin, Gulf of Mexico. *Geochim. Cosmochim. Acta* **187**, 1–20.

Zhuang G.-C., Lin Y.-S., Bowles M. W., Heuer V. B., Lever M. A., Elvert M. and Hinrichs K.-U. (2017) Distribution and isotopic composition of trimethylamine, dimethylsulfide and dimethylsulfoniopropionate in marine sediments. *Mar. Chem.* **196**, 35–46.

Zhuang G.-C., Lin Y.-S., Elvert M., Heuer V. B. and Hinrichs K.-U. (2014) Gas chromatographic analysis of methanol and ethanol in marine sediment pore waters: validation and implementation of three pretreatment techniques. *Mar. Chem.* **160**, 82–90.

Zhuang G.-C., Yang G.-P., Yu J. and Gao Y. (2011) Production of DMS and DMSP in different physiological stages and salinity conditions in two marine algae. *Chin. J. Oceanol. Limnol.* **29**, 369–377.

Associate editor: Edward Hornibrook